Impact of Off-nominal Frequency Values on the Generation Scheduling of Small-size Power Systems

Miguel Carrión[a,], Rafael Zárate-Miñano[b], Federico Milano[c]

[a]*Escuela de Ingeniería Industrial y Aeroespacial, UCLM, Toledo, Spain*
[b]*Escuela de Ingeniería Minera e Industrial, UCLM, Almadén, Spain*
[c]*School of Electrical and Electronic Engineering, University College Dublin, Ireland*

Abstract

This paper studies the impact of off-nominal steady-state frequency values on the generation scheduling of small-size power systems. For that, a security-constrained stochastic unit commitment problem that explicitly considers frequency variations and primary frequency control is proposed. The frequency of the system under normal operating conditions is characterized by a probability distribution that can be estimated from real-world measurements. The reserve scheduling is considered to face uncertain variations of renewable power and demand. A set of contingencies modeling generating unit failures is considered to ensure a N-1 security criterion. Numerical results obtained from a realistic case study show that modeling off-nominal steady-state frequency values in the scheduling model reduces the probability of experiencing high frequency deviations and unserved demand after contingency.

Keywords: renewable generation, primary frequency control, stochastic unit commitment, two-stage decision making.

Email addresses: Miguel.Carrion@uclm.es (Miguel Carrión), Rafael.Zarate@uclm.es (Rafael Zárate-Miñano), federico.milano@ucd.ie (Federico Milano)

1. Introduction

The main idea of this paper originates from the observation of the statistical distribution of the frequency in real-world systems. Figure 1 shows the histogram of frequency measurements acquired from the Irish power system during one week with a sampling ratio of 0.1 seconds. This figure shows that frequency is actually not equal to the synchronous one for most of the time, [1].

This situation may jeopardize the security of the system if a failure in a generating unit happens when the frequency is under its nominal value. In fact, this has become more and more an issue due to the high penetration of renewable energy resources in current power systems. In this sense, the increase of renewable production in the WECC system has been identified as the major cause of shortage of Primary Frequency Control (PFC) after contingencies, [2]. Moreover, it has been observed a reduction of the available amount of PFC in the US Eastern Interconnection from 37.5 MW/mHz in 1994 to 30.7 MW/mHz in 2004, [3]. With this regard, the European Parliament and the Council stated, through the so-called *Clean Energy for all Europeans* package, that electricity markets need to be improved to meet the needs of renewable energies, [4]. Furthermore, in this package, the following risk sources have been identified in the short-term operation of power systems: i) the uncertainty associated to unplanned outages of power plants, ii) the variation of the demand, and iii) the variability of the production of energy from renewable sources, [5].

In this paper, we analyze the influence of considering explicitly pre-contingency steady-state frequency deviations in the operation of a power system by formulating and solving a security-constrained unit commitment problem that takes into account both demand and intermittent power uncertainties as well as frequency fluctuations and unplanned outages of generation units.

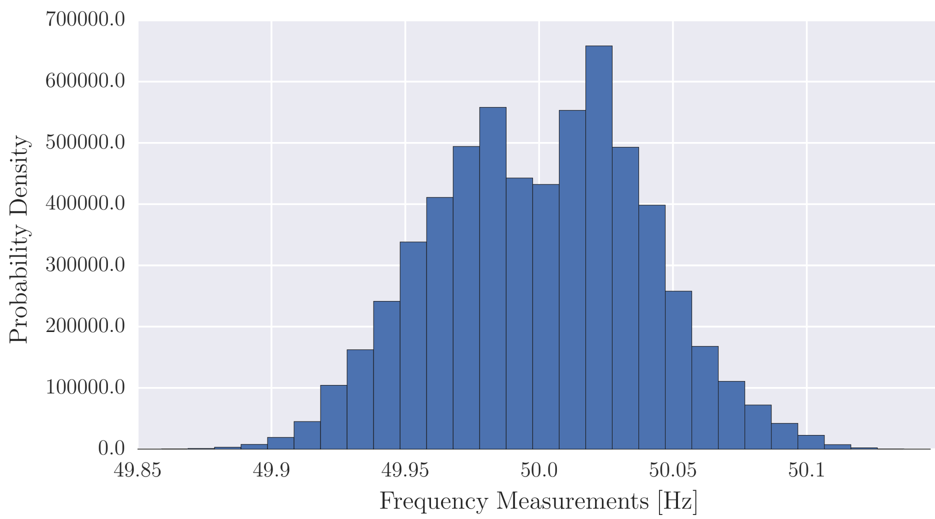

Figure 1: Histogram of the frequency of the Irish system from the 16th to the 22nd of December 2016.

A significant effort has been dedicated to study how to schedule simultaneously energy and reserve in power systems with high presence of intermittent power units. In this regard, [6] presents a security-constrained unit commitment algorithm in which a generation redispatch is considered for satisfying wind power variabilities in different scenarios. Reference [7] proposes an electricity market-clearing algorithm in which unit commitment and reserve needs are computed using a stochastic programming approach. In [8], a combined approach based on stochastic programming and a novel reserve quantification method is proposed. Reference [9] presents a two-stage stochastic programming problem for determining the reserve requirements in power systems with a large penetration of wind power. Reference [10] proposes a stochastic unit commitment formulation especially tailored for power system dominated by concentrating solar power plants and wind power units. The interested reader is referred to [11] for a complete review of stochastic unit commitment models. The operation of small and isolated power systems has been also analyzed in detail. For instance, the authors of [12] propose a risk-averse stochastic unit commitment for isolated power systems. Reserve requirements in isolated power systems are explicitly considered in the unit commitment formulation provided in [13]. A novel procedure to calculate the maximum wind power penetration in an isolated power system is presented in [14].

Several studies that focus on the unit commitment problem with frequency regulation constraints have been carried out in the last decade. The conventional approach on this topic is to take into account the effect of contingencies on frequency variations in order to determine the needs of reserve. With this aim, [15] considers the steady-state variation of the frequency following the contingency, whereas in [16] and [17] the constraint is based on the frequency nadir during the transient. Both methods need to take into account with various levels of approximation the power-frequency droop characteristic of the frequency control. A multi-period security-constrained economic dispatch model considering frequency stability constraints is developed in [18]. Reference [19] presents a mixed-integer linear formulation for the unit commitment problem considering that the frequency has to be greater than a lower limit in the event of a contingency. In the same vein, [20] provides a novel formulation for the unit commitment problem that accounts for failures of generating units and optimizes their droop coefficients for supplying primary frequency regulation. The usage of battery energy storages for frequency regulation in isolated power systems is studied in [21]. The frequency provision service by battery storage systems and electric vehicles has been studied in [23] and [24], respectively. Finally, a literature review on possible sources of non-synchronous fast frequency reserve is provided in [25].

A common feature of all papers cited above is that the frequency before the occurrence of the contingency is assumed to be equal to the nominal synchronous frequency. From the observation of Figure 1, however, we note that the value of the frequency is different from its nominal value (50 Hz) most of the time. This figure shows that the probability of experiencing a frequency greater than 50.05 Hz in the analyzed period is 16.6%, whereas the probability of the frequency to be less than 49.95 Hz is 9.0%. Hence, in this paper, we propose a novel approach where this fact is taken into account as a part of the scheduling problem. We then consider different scenarios according to the probability that the frequency is higher or lower than the synchronous one and solve the unit-commitment problem taking into account the effect of the primary frequency control.

In particular, the paper focuses on the short-term operation problem from the perspective of the system operator, considering a planning horizon spanning 24 hours. To avoid load shedding actions related to high variations of the frequency, it is of interest to take into account the participation of generating units in the frequency regulation service when deciding the commitment of the units. Additionally, the N-1 security criterion is imposed to ensure that there is no violations of the frequency limits if a single generating unit is removed from the system. Specifically, we formulate and solve a security-constrained stochastic unit commitment model to determine the day-ahead scheduling accounting for the modeling of the frequency under normal operating conditions. The proposed scheduling model is formulated as a two-stage stochastic programming problem. The first stage represents the day-ahead scheduling, while the second stage describes the multiple operation conditions that result from the uncertainty associated with (i) demand, (ii) renewable power output and (iii) steady-state pre- and post-contingency frequency of the system. It is important to emphasize that the resulting post-contingency frequency is not input data, but an output of the proposed model. The resulting problem is formulated as a large-scale mixed-integer linear programming problem. Although the proposed model can be used in large power systems, its application is of special interest for small-size power systems, which are more exposed to large frequency deviations.

The main contribution of this paper is a quantitative approach to evaluate the influence of the variability of the steady-state pre-contingency frequency in the day-ahead energy and reserve scheduling of a small-size power system. To perform this analysis, a linear formulation modeling the PFC of the generating units considering frequency deviations under normal operating conditions and after generating unit failures is proposed. This formulation is included in the stochastic unit commitment problem, which has been finally formulated as a two-stage stochastic programming problem that is solved using an iterative algorithm. Additionally, a realistic case study based on the isolated power system of Lanzarate and Fuerteventura in Spain is out to test the proposed procedure. The simulations performed in the case study reveal how the modeling of the steady-state pre-contingency frequency deviations in the day-ahead scheduling reduces the total expected costs in a large majority of the analyzed days, cuts down the unserved demand, and reduces the probability of experiencing high frequency deviations after contingency.

The rest of this paper is organized as follows: Section 2 describes the modeling of the PFC service and of the system frequency. Section 3 presents the mathematical formulation of the proposed security-constrained unit commitment model. Section 4 provides and analyzes a numerical case study, and Section 5 includes some relevant conclusions.

2. Rationale behind Frequency Variations

The main objective of the frequency regulation of a HV transmission system is to maintain the balance between the power produced by the generators and the power consumed by the loads at the rated frequency. To avoid large excursions of the system frequency following a disturbance, say ΔP_D, a PFC is included in every power plant capable to provide primary frequency regulation. Roughly speaking, this consists in a transfer function $G_f(s)$ that takes as input the rotor speed error ε_Ω, i.e., the difference between the synchronous speed Ω^{ref} and the instantaneous machine rotor speed Ω and imposes to the machine the required mechanical power ΔP_g to reduce such a frequency error.

Standard turbine governor transfer functions $G_f(s)$ do not perfectly track the frequency and, thus, $\varepsilon_\Omega \neq 0$ in steady-state. Assuming per unit quantities $\Delta\Omega = \Delta f$, where Δf is the variation of the frequency of the system. Then, for a given unit g, the steady-state characteristic of the PFC is given by:

$$\Delta f = -R_g \Delta P_g \tag{1}$$

where ΔP_g and R_g are, respectively, the variation of the power output and the droop of unit g. Equation (1) is for a single machine. The system droop is given by:

$$\frac{1}{R} = \frac{1}{P_N} \sum_g \frac{P_{N,g}}{R_g} \tag{2}$$

where $P_{N,g}$ is the nominal capacity of unit g and $P_N = \sum_g P_{N,g}$ is the total capacity of the system. Neglecting losses, and according to (2), the frequency variation in steady state for a net load deviation ΔP_D is:

$$\Delta f = -R \Delta P_D \tag{3}$$

from where it can observed that the frequency variation in steady state only depends on the parameter R and the variation on the total electrical power demand ΔP_D.

In most large interconnected systems, the secondary frequency control or automatic generation control (AGC), is utilized to remove the frequency steady-state error due to the PFC through an appropriate rescheduling of generating units. To ensure stability, however, the AGC is much slower than the PFC. This leads to the fact that, for a considerable amount of time, the frequency of the system is actually not the synchronous one.

The system frequency can be measured and characterized afterwards using standard statistical techniques. In this way, the frequency distribution can be discretized so that a frequency value and a probability is assigned to each discretization point. For example, Figure 2 provides two different 7-point discretizations of the frequency under normal operating conditions. Figure 2a corresponds to a bimodal distribution, whereas a unimodal distribution is characterized in Figure 2b. Note that the bimodal distribution of the frequency has been observed in systems with non-automatic secondary frequency control, [1].

3. Formulation

3.1. Decision-Making Framework

In this paper, we consider a market clearing procedure in which the scheduling and dispatch of energy is performed in a two-step procedure. This type of clearing procedure is especially tailored for power systems with a high penetration of intermittent units [11]. The main advantage of co-optimizing simultaneously energy and reserve capacity is that it is possible to determine a day-ahead schedule that is flexible enough to accommodate effectively the volatility of loads and intermittent power outputs. We assume that the unit commitment and the scheduling of energy and spinning reserve capacity are determined in the day-ahead market. We also consider that this reserve capacity is dedicated to deploy the operating reserve used to follow deviations of intermittent production and demand.

When electricity is physically delivered, the real-time dispatch is performed to determine the reserve deployments needed to counter possible deviations from the scheduled energy quantities. At this time, the PFC is also performed if short-term net load fluctuations occur. Additionally, it is also

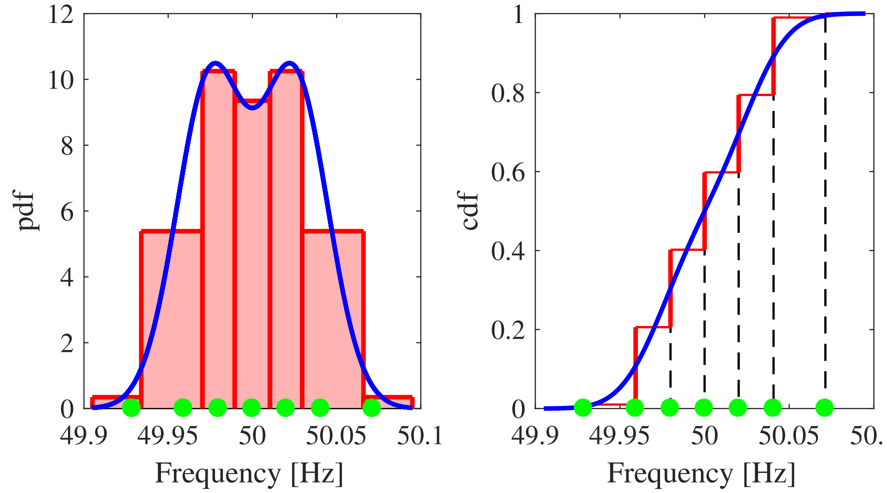

(a) 7-point discretization of the frequency characterized by a bimodal normal distribution with parameters $\mu_1 = 49.975$, $\mu_2 = 50.025$ and $\sigma_1 = \sigma_2 = 0.025$ Hz.

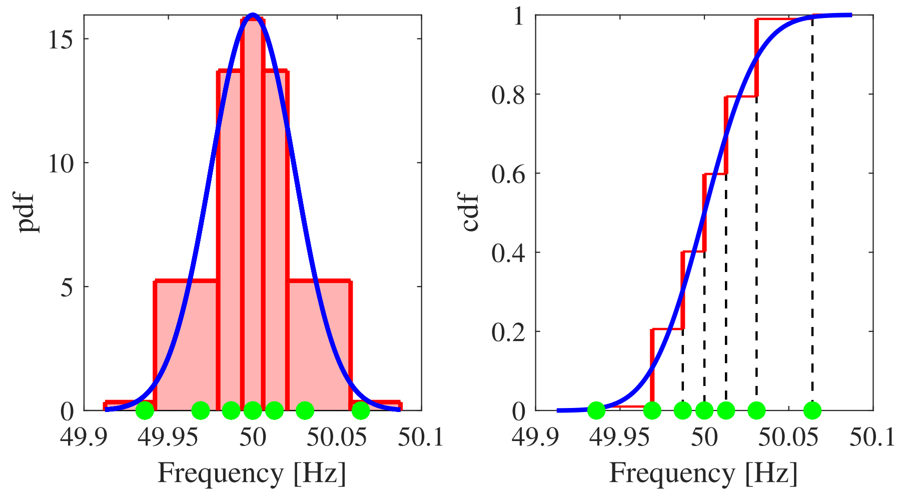

(b) 7-point discretization of the frequency characterized by a unimodal normal distribution with parameters $\mu = 50$ and $\sigma = 0.025$ Hz.

Figure 2: Frequency distribution discretization.

considered that if an unexpected failure occurs in a generating unit, all committed and dispatchable units must provide PFC in order to maintain the system frequency within adequate levels.

From a mathematical point of view, the day-ahead market clearing described above is a security-constrained stochastic unit commitment formulated as a two-stage stochastic programming problem in which the first-stage represents the day-ahead market, while the second-stage represents the real-time dispatch.

Three uncertain parameters are considered in this problem, namely: i) hourly intermittent power production, ii) hourly system demand and iii) steady-state frequency fluctuations. These uncertain parameters are characterized as stochastic processes which can be discretized into a set of scenarios [26]. Each scenario is a plausible realization of the stochastic processes. Different scenario generation procedures for modeling these uncertain parameters are provided in [27]. The failures of generating units are modeled by means of a set of possible contingencies, where each contingency has associated an occurrence probability. The decision-making process described above is provided in Figure 3.

Finally, since this paper is dealing with a day-ahead scheduling problem, the transient behaviour of the frequency is not modeled and only steady-state values are considered.

3.2. Notation

The notation used in this section is provided below. Symbols referring to parameters and variables are denoted using capital and lowercase letters, respectively. Note that two scenario indices are used: index ω refers to scenarios modeling system demand and intermittent power production whereas index ξ refers to scenarios modeling pre-contingency frequency values.

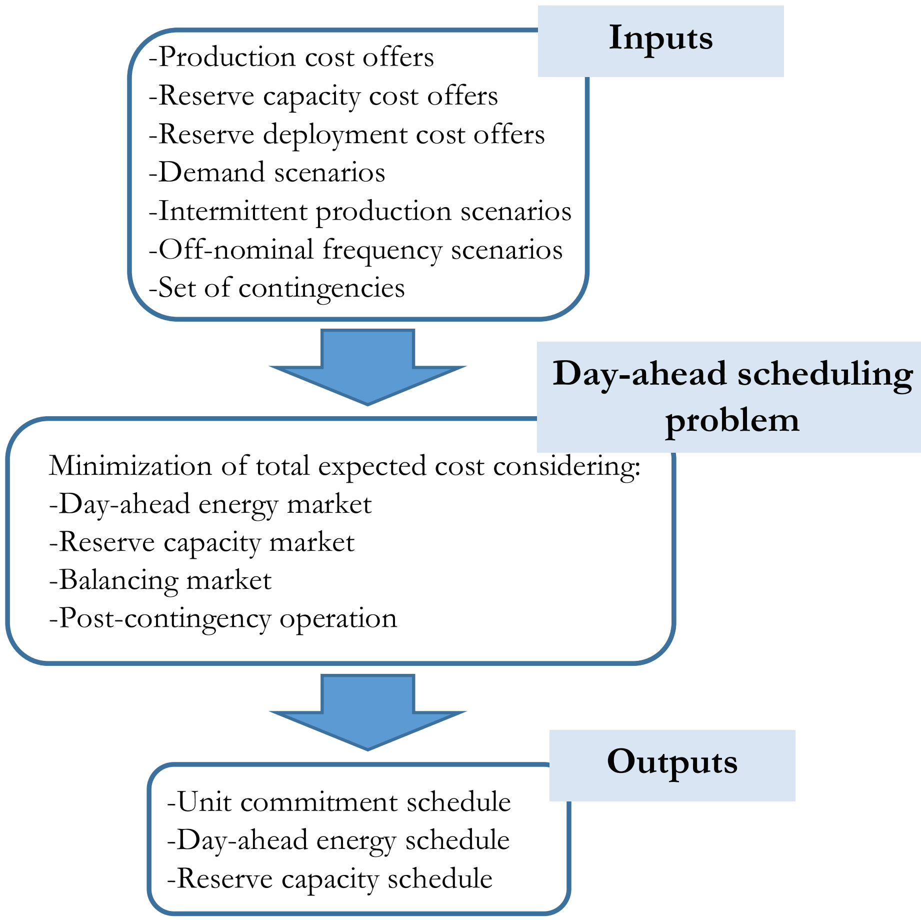

Figure 3: Procedure flowchart.

Indices and sets

c/C Index/set of contingencies

g/G Index/set of generating units

G_n Set of generating units located in bus n

$G^{\mathrm{D/I}}$ Set of dispatchable/intermittent generating units

$G_n^{\mathrm{D/I}}$ Set of dispatchable/intermittent generating units located in bus n

G^{F} Set of dispatchable generating units capable to provide PFC

ℓ/L Index/set of transmission lines

L_n^{O} Set of lines whose origin bus is n

L_n^{F} Set of lines whose destination bus is n

n/N Index/set of buses

t/T Index/set of time periods

ω/Ω Index/set of scenarios used for modeling demand and intermittent power availability

ξ/Ξ Index/set of scenarios used for modeling the pre-contingency state frequency

Ξ^{OS} Set of out-of-sample scenarios used for modeling the pre-contingency state frequency

Variables

$c_{gt}^{\mathrm{U/D}}$ Scheduled up/down reserve capacity in the day-ahead market by unit g in period t

$c_{gt}^{\mathrm{SU/SD}}$ Startup/Shutdown cost of unit g in period t

p_{gt}^{D} Power scheduled in the day-ahead market by unit g in period t

$p_{gt\omega}^{\mathrm{G}}$ Power generated by unit g in period t and scenario ω

$p_{gt\omega\xi c}^{\mathrm{G,PC}}$ Variation of the power generated by unit g in period t and scenarios ω and ξ in post-contingency state c

$p_{gt\omega\xi}^{\mathrm{G},\Delta}$ Primary reserve output of unit g in period t and scenarios ω and ξ

$p_{gt\omega\xi}^{\mathrm{GS,F}}$ Forced power spillage of intermittent unit g in period t and scenarios ω and ξ

$p_{\ell t}^{\mathrm{L,D}}$ Power flow resulting from the day-ahead schedule in line ℓ and period t

$p_{\ell t\omega}^{\mathrm{L,RT}}$ Power flow resulting from the real-time dispatch in line ℓ, period t and scenario ω

$p_{nt\omega}^{\mathrm{UD}}$ Unserved demand in the real-time dispatch in bus n, period t and scenario ω

$p_{nt\omega\xi}^{\mathrm{UD,F}}$ Unserved demand resulting from the primary frequency control in bus n, period t and scenarios ω and ξ

$p_{nt\omega\xi c}^{\mathrm{UD,PC}}$ Unserved demand resulting from contingency c, in bus n, period t and scenarios ω and ξ

$r^{\mathrm{U/D}}_{gt\omega}$ Deployed up/down scheduled reserve in the real-time dispatch by unit g in period t and scenario ω

v_{gt} Binary variable modeling the commitment of unit g in period t, being equal to 1 if the unit g is on line, and 0 otherwise

$\Delta f^{\mathrm{PC}}_{t\omega\xi c}$ System frequency variation in post-contingency state in period t, scenarios ω and ξ and post-contingency state c

$\Delta f_{t\omega\xi}$ System frequency variation in pre-contingency state in period t and scenarios ω and ξ

θ^{D}_{nt} Voltage bus angle resulting from the day-ahead schedule in bus n and period t

$\theta^{\mathrm{RT}}_{nt\omega}$ Voltage bus angle resulting from the real-time dispatch in bus n, period t and scenario ω

Parameters

$C^{\mathrm{CU/CD}}_{g}$ Up/down reserve capacity cost offer of unit g

C^{D}_{g} Production cost offer of unit g in the day-ahead market

$C^{\mathrm{DU/DD}}_{g}$ Deployed up/down reserve cost offer of unit g

$C^{\mathrm{GS,F}}$ Cost of forced intermittent power spillage

$C^{\mathrm{SU/SD}}_{g}$ Startup/Shutdown cost parameter of unit g

$C^{\mathrm{U/D}}_{\max,gt}$ Upper limit of scheduled up/down reserve by unit g in period t

C^{UD} Cost of unserved energy

O_ℓ/F_ℓ Origin/Destination bus of line ℓ

$P^{\mathrm{D,D}}_{nt}$ Power demand in the day-ahead market in bus n and period t

$P^{\mathrm{D,RT}}_{nt\omega}$ Power demand in the real-time dispatch in bus n, period t and scenario ω

$P^{\mathrm{D},\Delta}_{S,t\omega\xi}$ Unexpected variation of the net system demand in the real-time dispatch in period t and scenarios ω and ξ

$P^{\mathrm{G}}_{\mathrm{max},g}$ Capacity of unit g

$P^{\mathrm{G}}_{\mathrm{min},g}$ Minimum power output of unit g

$P^{\mathrm{G}}_{\mathrm{su/sd},g}$ Startup/Shutdown ramp limit of unit g

$P^{\mathrm{G}}_{\mathrm{up/dw},g}$ Ramp-up/down limit of unit g

$P^{\mathrm{L}}_{\mathrm{max},\ell}$ Capacity of line ℓ

R_g Parameter used to determine the droop of generating unit g

$U^{\mathrm{I,D}}_{gt}$ Availability of intermittent unit g in the day-ahead market in period t

$U^{\mathrm{I,RT}}_{gt\omega}$ Availability of intermittent unit g in the real-time dispatch in period t and scenario ω

U^{PC}_{gc} Availability parameter that is equal to 0 if outage of unit g occurrs in contingency c, being 1 otherwise

X_ℓ Reactance of line ℓ

$\Delta f_{\max}$ Maximum system frequency variation allowed

π_ω Probability of scenario ω

ρ_ξ Probability of scenario ξ

τ_c Probability of contingency c

3.3. Security-constrained stochastic unit commitment formulation

The mathematical formulation of the security-constrained stochastic unit commitment problem is provided below. The proposed model differs from traditional security-constrained unit commitment models in the sense that energy and up and down reserve capacities are co-optimized in the first stage. This type of scheduling is appropriate for those power systems with a high penetration of renewable units [22]. If energy and reserve capacities are simultaneously optimized, it is possible to determine a day-ahead schedule that is flexible enough to effectively accommodate the uncertain and variable power output of intermittent units. This scheduling problem is formulated as a classical two-stage stochastic programming problem in which the first-stage represents the day-ahead market, while the second-stage represents the actual energy deployment in which uncertain parameters are revealed and reserves are deployed.

$$\text{Minimize}_{\Theta}$$

$$\sum_{t\in T}\sum_{g\in G}\left(c_{gt}^{\mathrm{SU}} + c_{gt}^{\mathrm{SD}} + C_g^{\mathrm{D}} p_{gt}^{\mathrm{D}} + C_g^{\mathrm{CU}} c_{gt}^{\mathrm{U}} + C_g^{\mathrm{CD}} c_{gt}^{\mathrm{D}}\right) +$$

$$\sum_{\omega\in\Omega}\pi_\omega\sum_{t\in T}\left(\sum_{g\in G^{\mathrm{D}}}\left(C_g^{\mathrm{DU}}r_{gt\omega}^{\mathrm{U}}-C_g^{\mathrm{DD}}r_{gt\omega}^{\mathrm{D}}\right)+\right.$$
$$\sum_{n\in N}C^{\mathrm{UD}}p_{nt\omega}^{\mathrm{UD}}+\sum_{\xi\in\Xi}\rho_\xi\left(\sum_{g\in G^{\mathrm{I}}}C^{\mathrm{GS,F}}p_{gt\omega\xi}^{\mathrm{GS,F}}+\right.$$
$$\left.\left.\sum_{n\in N}C^{\mathrm{UD}}\left(p_{nt\omega\xi}^{\mathrm{UD,F}}+\sum_{c\in C}\tau_c p_{nt\omega\xi c}^{\mathrm{UD,PC}}\right)\right)\right) \tag{4}$$

Subject to:

(Startup and shutdown costs)

$$c_{gt}^{\mathrm{SU}}\geq C_g^{\mathrm{SU}}\left(v_{gt}-v_{gt-1}\right),\quad \forall g\in G^{\mathrm{D}},\forall t\in T \tag{5}$$
$$c_{gt}^{\mathrm{SD}}\geq C_g^{\mathrm{SD}}\left(v_{gt-1}-v_{gt}\right),\quad \forall g\in G^{\mathrm{D}},\forall t\in T \tag{6}$$
$$c_{gt}^{\mathrm{SU}}\geq 0,\ c_{gt}^{\mathrm{SD}}\geq 0,\quad \forall g\in G,\forall t\in T \tag{7}$$

(Reserve capacity scheduling)

$$0\leq c_{gt}^{\mathrm{U}}\leq C_{\max,gt}^{\mathrm{U}}v_{gt},\quad \forall g\in G^{\mathrm{D}},\forall t\in T \tag{8}$$
$$0\leq c_{gt}^{\mathrm{D}}\leq C_{\max,gt}^{\mathrm{D}}v_{gt},\quad \forall g\in G^{\mathrm{D}},\forall t\in T \tag{9}$$

(Power limits of generating units in the day-ahead market)

$$P_{\min,g}^{\mathrm{G}}v_{gt}\leq p_{gt}^{\mathrm{D}}\leq P_{\max,g}^{\mathrm{G}}v_{gt},\quad \forall g\in G^{\mathrm{D}},\forall t\in T \tag{10}$$
$$0\leq p_{gt}^{\mathrm{D}}\leq U_{gt}^{\mathrm{I,D}}P_{\max,g}^{\mathrm{G}},\quad \forall g\in G^{\mathrm{I}},\forall t\in T \tag{11}$$

(Power ramps of the units in the day-ahead market)

$$\begin{aligned} p_{gt}^{\mathrm{D}} - p_{gt-1}^{\mathrm{D}} \leq P_{\mathrm{up},g}^{\mathrm{G}} v_{gt-1} + P_{\mathrm{su},g}^{\mathrm{G}} \left(v_{gt} - v_{gt-1}\right) \\ + \left(1 - v_{gt}\right) P_{\mathrm{max},g}^{\mathrm{G}}, \quad \forall g \in G^{\mathrm{D}}, \forall t \in T \end{aligned} \tag{12}$$

$$\begin{aligned} p_{gt-1}^{\mathrm{D}} - p_{gt}^{\mathrm{D}} \leq P_{\mathrm{dw},g}^{\mathrm{G}} v_{gt} + P_{\mathrm{sd},g}^{\mathrm{G}} \left(v_{gt-1} - v_{gt}\right) \\ + \left(1 - v_{gt-1}\right) P_{\mathrm{max},g}^{\mathrm{G}}, \quad \forall g \in G^{\mathrm{D}}, \forall t \in T \end{aligned} \tag{13}$$

(Power flow constraints in the day-ahead market)

$$p_{\ell t}^{\mathrm{L,D}} = \frac{1}{X_\ell} \left(\theta_{O_\ell t}^{\mathrm{D}} - \theta_{F_\ell t}^{\mathrm{D}}\right), \quad \forall \ell \in L, \forall t \in T \tag{14}$$

$$-P_{\mathrm{max},\ell}^{\mathrm{L}} \leq p_{\ell t}^{\mathrm{L,D}} \leq P_{\mathrm{max},\ell}^{\mathrm{L}}, \quad \forall \ell \in L, \forall t \in T \tag{15}$$

(Power balance in the day-ahead market)

$$\sum_{g \in G_n} p_{gt}^{\mathrm{G}} - \sum_{\ell \in L_n^{\mathrm{O}}} p_{\ell t}^{\mathrm{L,D}} + \sum_{\ell \in L_n^{\mathrm{F}}} p_{\ell t}^{\mathrm{L,D}} = P_{nt}^{\mathrm{D,D}}, \quad \forall n \in N, \forall t \in T \tag{16}$$

(Reserve deployment in the real-time dispatch)

$$0 \leq r_{gt\omega}^{\mathrm{U}} \leq c_{gt}^{\mathrm{U}}, \quad \forall g \in G^{\mathrm{D}}, \forall t \in T, \forall \omega \in \Omega \tag{17}$$

$$0 \leq r_{gt\omega}^{\mathrm{D}} \leq c_{gt}^{\mathrm{D}}, \quad \forall g \in G^{\mathrm{D}}, \forall t \in T, \forall \omega \in \Omega \tag{18}$$

(Power limits of generating units in the real-time dispatch)

$$\begin{aligned} p_{gt\omega}^{\mathrm{G}} = p_{gt}^{\mathrm{D}} + r_{gt\omega}^{\mathrm{U}} - r_{gt\omega}^{\mathrm{D}}, \\ \forall g \in G^{\mathrm{D}}, \forall t \in T, \forall \omega \in \Omega \end{aligned} \tag{19}$$

$$P^{\mathrm{G}}_{\min,g} v_{gt} \leq p^{\mathrm{G}}_{gt\omega} \leq P^{\mathrm{G}}_{\max,g} v_{gt},$$
$$\forall g \in G^{\mathrm{D}}, \forall t \in T, \forall \omega \in \Omega \tag{20}$$
$$0 \leq p^{\mathrm{G}}_{gt\omega} \leq U^{\mathrm{I,RT}}_{gt\omega} P^{\mathrm{G}}_{\max,g},$$
$$\forall g \in G^{\mathrm{I}}, \forall t \in T, \forall \omega \in \Omega \tag{21}$$

(Power ramps of generating units in the real-time dispatch)

$$p^{\mathrm{G}}_{gt\omega} - p^{\mathrm{G}}_{gt-1,\omega} \leq P^{\mathrm{G}}_{\mathrm{up},g} v_{gt-1} + P^{\mathrm{G}}_{\mathrm{su},g} \left(v_{gt} - v_{gt-1}\right)$$
$$+ \left(1 - v_{gt}\right) P^{\mathrm{G}}_{\max,g},\ \forall g \in G^{\mathrm{D}}, \forall t \in T, \forall \omega \in \Omega \tag{22}$$
$$p^{\mathrm{G}}_{gt-1,\omega} - p^{\mathrm{G}}_{gt\omega} \leq P^{\mathrm{G}}_{\mathrm{dw},g} v_{gt} + P^{\mathrm{G}}_{\mathrm{sd},g} \left(v_{gt-1} - v_{gt}\right)$$
$$+ \left(1 - v_{gt-1}\right) P^{\mathrm{G}}_{\max,g}, \forall g \in G^{\mathrm{D}}, \forall t \in T, \forall \omega \in \Omega \tag{23}$$

(Power flow constraints in the real-time dispatch)

$$p^{\mathrm{L,RT}}_{\ell t\omega} = \frac{1}{X_\ell} \left(\theta^{\mathrm{RT}}_{O_\ell t\omega} - \theta^{\mathrm{RT}}_{F_\ell t\omega}\right), \quad \forall \ell \in L, \forall t \in T, \forall \omega \in \Omega \tag{24}$$
$$-P^{\mathrm{L}}_{\max,\ell} \leq p^{\mathrm{L,RT}}_{\ell t\omega} \leq P^{\mathrm{L}}_{\max,\ell}, \quad \forall \ell \in L, \forall t \in T, \forall \omega \in \Omega \tag{25}$$

(Power balance in the real-time dispatch)

$$\sum_{g \in G^{\mathrm{D}}_n} \left(r^{\mathrm{U}}_{gt\omega} - r^{\mathrm{D}}_{gt\omega}\right) + \sum_{g \in G^{\mathrm{I}}_n} \left(p^{\mathrm{G}}_{gt\omega} - p^{\mathrm{D}}_{gt}\right)$$
$$- \sum_{\ell \in L^{\mathrm{O}}_n} \left(p^{\mathrm{L,RT}}_{\ell t\omega} - p^{\mathrm{L,D}}_{\ell t}\right) + \sum_{\ell \in L^{\mathrm{F}}_n} \left(p^{\mathrm{L,RT}}_{\ell t\omega} - p^{\mathrm{L,D}}_{\ell t}\right) + p^{\mathrm{UD}}_{nt\omega}$$
$$= P^{\mathrm{D,RT}}_{nt\omega} - P^{\mathrm{D,D}}_{nt}, \quad \forall n \in N, \forall t \in T, \forall \omega \in \Omega \tag{26}$$

(Pre-contingency frequency regulation constraints)

$$0 \leq p^{\mathrm{G},\Delta}_{gt\omega\xi} \leq -\frac{1}{R_g}\Delta f_{t\omega\xi},$$
$$\forall g \in G^{\mathrm{F}}, \forall t \in T, \forall \omega \in \Omega, \forall \xi \in \Xi, \mathrm{if}\, P^{\mathrm{D},\Delta}_{\mathrm{S},t\omega\xi} \geq 0 \tag{27}$$

$$-\frac{1}{R_g}\Delta f_{t\omega\xi} \leq p^{\mathrm{G},\Delta}_{gt\omega\xi} \leq 0,$$
$$\forall g \in G^{\mathrm{F}}, \forall t \in T, \forall \omega \in \Omega, \forall \xi \in \Xi, \mathrm{if}\, P^{\mathrm{D},\Delta}_{\mathrm{S},t\omega\xi} \leq 0 \tag{28}$$

$$\sum_{g \in G^{\mathrm{F}}} p^{\mathrm{G},\Delta}_{gt\omega\xi} + \sum_{n \in N} p^{\mathrm{UD,F}}_{nt\omega\xi} - \sum_{g \in G^{\mathrm{I}}} p^{\mathrm{GS,F}}_{gt\omega\xi} = p^{\mathrm{D},\Delta}_{\mathrm{S},t\omega\xi},$$
$$\forall t \in T, \forall \omega \in \Omega, \forall \xi \in \Xi \tag{29}$$

$$0 \leq p^{\mathrm{GS,F}}_{gt\omega\xi} \leq P^{\mathrm{G}}_{gt\omega},$$
$$\forall g \in G^{\mathrm{I}}, \forall t \in T, \forall \omega \in \Omega, \forall \xi \in \Xi \tag{30}$$

(Post-contingency frequency regulation constraints)

$$0 \leq p^{\mathrm{G,PC}}_{gt\omega\xi c} \leq -\frac{1}{R_g}\Delta f^{\mathrm{PC}}_{t\omega\xi c}, \quad \forall g \in G^{\mathrm{F}}, \forall t \in T,$$
$$\forall c \in C, \forall \omega \in \Omega, \forall \xi \in \Xi, \mathrm{if}\, U^{\mathrm{PC}}_{gc} = 1 \tag{31}$$

$$P^{\mathrm{G}}_{\min,g} v_{gt} \leq p^{\mathrm{G}}_{gt\omega} + p^{\mathrm{G},\Delta}_{gt\omega\xi} + p^{\mathrm{G,PC}}_{gt\omega\xi c} \leq P^{\mathrm{G}}_{\max,g} v_{gt},$$
$$\forall c \in C, \forall g \in G^{\mathrm{F}}, \forall t \in T, \forall \omega \in \Omega, \forall \xi \in \Xi, \mathrm{if}\, U^{\mathrm{PC}}_{gc} = 1 \tag{32}$$

$$p^{\mathrm{G}}_{gt\omega} + p^{\mathrm{G},\Delta}_{gt\omega\xi} + p^{\mathrm{G,PC}}_{gt\omega\xi c} = 0, \quad \forall c \in C, \forall g \in G,$$
$$\forall t \in T, \forall \omega \in \Omega, \forall \xi \in \Xi, \mathrm{if}\, U^{\mathrm{PC}}_{gc} = 0 \tag{33}$$

$$\sum_{g \in G} p^{\mathrm{G,PC}}_{gt\omega\xi c} - p^{\mathrm{UD,PC}}_{nt\omega\xi c} = 0,$$
$$\forall c \in C, \forall t \in T, \forall n \in N, \forall \omega \in \Omega, \forall \xi \in \Xi \tag{34}$$

$$-\Delta f_{\max} \leq \Delta f^{\mathrm{PC}}_{t\omega\xi c} + \Delta f_{t\omega\xi} \leq \Delta f_{\max},$$
$$\forall c \in C, \forall t \in T, \forall \omega \in \Omega, \forall \xi \in \Xi \tag{35}$$

The objective function (4) formulates the expected costs considering startup and shutdown costs, generating costs associated with the day-ahead market, up and down reserve capacity costs, up and down reserve deployment expected costs, and load shed and forced wind spillage expected costs.

Constraints (5)-(7) model the startup and shutdown costs. Constraints (8)-(9) establish the limits of the reserve capacities that can be provided by each unit. It is considered that those units defined as intermittent units, ($g \in G^{\mathrm{I}}$), are not able to provide reserve services. The power limits of the generating units are established by constraints (10) and (11). Observe that the power production of intermittent units is bounded by the availability factor $U_{gt}^{\mathrm{R,D}}$ which value ranges between 0 and 1. The power ramps of generating units in the day-ahead market are formulated by constraints (12) and (13). Constraints (14) and (15) formulate the line power flows in the day-ahead market. The power balance in the day-ahead market is established by constraints (16).

The deployed up and down spinning reserves are bounded by constraints (17) and (18), respectively. Constraints (19) compute the total power generated by each dispatchable unit as the sum of the power committed in the day-ahead market and the reserve deployments in the real-time dispatch. The power limits of conventional and intermittent power units in the real-time dispatch are established by constraints (20) and (21), respectively. The power ramps of generating units in the real-time dispatch are expressed by constraints (22) and (23). Constraints (24) and (25) are used to compute the resulting line power flows from the real-time dispatch. Constraints (26) establish the power balance in the real-time dispatch.

Constraints (27)-(30) are proposed to model the PFC of the generating units under normal operating conditions in the pre-contingency state. A generating unit can provide PFC only if it is committed, i.e. $v_{gt} = 1$, and its participation depends on i) the droop of the unit, R_g, and ii) the pre-contingency frequency variation, $\Delta f_{t\omega\xi}$. Constraints (27) are referred to the case in which a positive net load power fluctuation occurs. Net load power fluctuations are modeled by parameter $P^{\mathrm{D},\Delta}_{\mathrm{S},t\omega\xi}$, which is equal to the product of the inverse of the system droop R times the frequency variation considered in each scenario. In this case, a committed generating unit g will increase its power output a quantity $p^{\mathrm{G},\Delta}_{gt\omega\xi}$ within the interval $0 \leq p^{\mathrm{G},\Delta}_{gt\omega\xi} \leq -\frac{1}{R_g}\Delta f_{t\omega\xi}$. Analogously, negative net load power fluctuation are considered by constraints (28). The power balance in the frequency regulation service is formulated through constraints (29). Note that the net-load deviations can be compensated by i) the PFC of the generating units ($p^{\mathrm{G},\Delta}_{gt\omega\xi}$), ii) the load shedding ($p^{\mathrm{UD,F}}_{nt\omega\xi}$) and the forced intermittent power spillage ($p^{\mathrm{GS,F}}_{gt\omega\xi}$). Finally, the upper and lower bounds to forced wind spillage are established by constraints (30).

The PFC in the post-contingency states is formulated by constraints (31)-(35). Post-contingency states are indexed by $c \in C$. The state referred as $c = 0$ indicates a post-contingency state where all committed units are at usage. The rest of states, $c > 0$, are used to characterize contingencies representing single failures of generating units. To that end, parameter $U^{\mathrm{PC}}_{gc} \in \{0, 1\}$ is used to model the availability of generating units. In this manner, U^{PC}_{gc} is equal to 0 if unit g suffers an unexpected failure in post-contingency state c. On the contrary, if $U^{\mathrm{PC}}_{gc} = 1$, it is considered that unit g is available in post-contingency state c. Considering this, constraints (31) and (32) are used to bound the increment of the power output of those committed units that do not suffer contingencies. Conversely, constraints (33) enforce that committed units that suffer a contingency must decrease their power production a value equal to its power output in the pre-contingency state. Constraints (34) establish the power balance in the post-contingency state. Finally, constraints (35) establish bounds to the frequency variations in the pre- and post-contingency states.

The main difference of formulation (4)-(35) with respect to other models is that off-nominal frequency variations in the pre-contingency state are explicitly considered through constraints (27)-(30). Additionally, the impact of pre-contingency frequency variations on the system frequency resulting after each considered contingency is formulated through constraints (31)-(35).

Observe that the large computational size of problem (4)-(35) avoids to solve it directly in real case studies using commercial solvers. For this reason, the solution procedure described in [24] is applied. This procedure is based on the fact that there exists a minimum set of contingencies over which it is sufficient to solve problem (4)-(35) to achieve the same solution than that obtained by solving the original problem, [28]. Therefore, it is possible to use an iterative procedure to solve the original problem (4)-(35) incorporating successively those contingencies that cause the greatest load shed in each iteration. The solution algorithm comprises the following steps:

- Step 0: Initialization. The set of active contingencies is initialized, including the no-contingency scenario.
- Step 1: Problem (4)-(35) is solved considering only the active set of contingencies. Since a reduced number of contingencies is considered,

the optimal objective function resulting from solving the problem with the active set of contingencies constitutes a lower bound of problem (4)-(35). Note that this problem is much faster to solve than the original problem since only a subset of contingencies is considered.

- Step 2: Problem (4)-(35) is solved considering the full set of contingencies and fixing the first-stage variables to the optimal values obtained in Step 1. Note that this problem is easy to solve because first-stage variables are fixed. The optimal objective function of this problem constitutes an upper bound of problem (4)-(35).

- Step 3: Convergence checking. The difference between the lower and upper bounds computed in Steps 1 and 2 is checked. If this difference is smaller than a specified tolerance, the solution procedure stops, the value of the objective function of problem (4)-(35) is equal to the upper bound, and the solution corresponds to the first-stage decision variables obtained in Step 1. If not, the set of active contingencies is updated adding the contingency that causes the greatest load shed and the algorithm returns back to Step 1.

We refer the interested reader to [24] for further details about this solution procedure.

4. Numerical results

The model proposed in Section 3.3 has been tested on a realistic case study based on the isolated power system of Lanzarote and Fuerteventura

(LZ-FV) belonging to the Canary Islands, Spain. Detailed information about this power system can be found in [12].

4.1. General input data

The power system considered comprises 8 lines, 25 thermal units, 5 wind units and 8 solar photovoltaic (PV) units. We assume that wind and PV power units are intermittent units, whereas the rest of units corresponds to dispatchable units that can participate in PFC. The technical characteristics of generating units are described in [12]. The load shed and forced wind spillage costs are equal to €5000/MWh.

All dispatchable units have a regulation droop of 5%, with a system nominal frequency of 50 Hz. The maximum allowed frequency variation is indicated afterwards for each solved instance. The frequency of the system is assumed to follow a bimodal distribution with parameters $\mu_1 = 49.975$, $\mu_2 = 50.025$ and $\sigma_1 = \sigma_1 = 0.025$ Hz and it has been discretized using three points with values $\{49.956, 50.000, 50.044\}$ and probabilities $\{0.17, 0.66, 0.17\}$, respectively. Observe that the proposed procedure allows to use any frequency distribution. The forced outage rate of thermal units is 3%. A system droop equal to 24.9 MW/Hz has been considered to compute the net demand variations associated with the frequency deviations in each period.

Based on the Lanzarote-Fuerteventura power system data for May 15th of 2015 [29], an initial set of 200 scenarios is generated to model system demand values as well as wind and solar PV power availabilities. This set has been reduced up to 10 scenarios using the fast forward scenario reduction algorithm presented in [30]. The resulting scenarios of demand, wind and solar PV availabilities are represented in Figure 4. The initial set of scenarios is depicted using light blue color, whereas dark blue color denotes the selected scenarios.

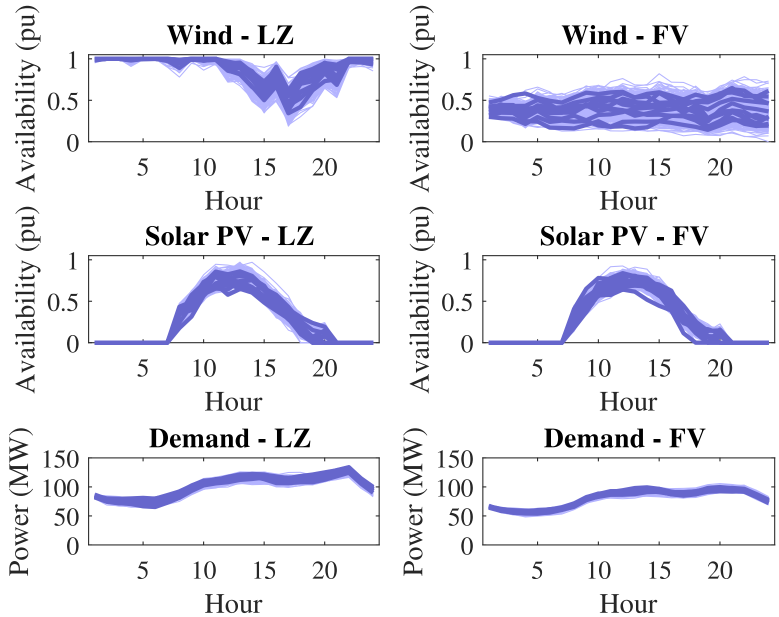

Figure 4: Scenarios.

4.2. Results

For the sake of comparison, two different models are considered:

- Model SCSUC+FD: This model corresponds to the proposed security-constrained stochastic unit commitment problem (4)-(35).

- Model SCSUC. This model does not consider pre-contingency frequency deviations in the day-ahead market scheduling, and it is equivalent to model SCSUC+FD without frequency regulation constraints (27)-(30) and enforcing $p^{\mathrm{G},\Delta}_{gt\omega\xi} = 0$ and $\Delta f_{t\omega\xi} = 0$.

In favor of comparing fairly the goodness of both models, an alternative set of 100 scenarios for modeling pre-contingency frequency deviations has been generated to perform an out-of-sample analysis. In this manner, all decisions corresponding to the unit commitment, day-ahead energy and spinning reserve capacity and energy scheduling variables are fixed to the optimal values obtained using the initial set of scenarios. Afterwards, each of the 100 scenarios is evaluated to determine the PFC decisions considering frequency deviations and unit contingencies.

The performance of models SCSUC+FD and SCSUC is analyzed by solving four different cases. These cases are built using two values of the maximum frequency variation, $\Delta f_{\max} = \{0.50, 0.25\}$ Hz, and two values of the renewable penetration factor (RPF) installed in the system, RPF= $\{1, 5\}$. The value of $\Delta f_{\max} = 0.50$ Hz considered in this case study is the maximum steady-state frequency deviation allowed in countries as Ireland or UK. Moreover, $\Delta f_{\max} = 0.25$ Hz is the maximum steady-state frequency deviation allowed by the Spanish system operator under normal operation conditions in non-mainland power systems, such as the system considered in this case study. The case RPF=1 considers the actual installed capacity of wind and solar PV units in 2015. On the other hand, case RPF=5 considers 5 times the capacity of wind and solar PV units indicated in 2015. All cases are solved applying the iterative procedure indicated in Section 3.3 and using CPLEX 12.2.0.1 under GAMS on a Linux-based server with four 2.9 GHz processors and 250 GB of RAM. The iterative process used to solve the problem stops if a relative error smaller than 0.1% is achieved.

Table 1 provides the resulting expected costs from solving the 4 cases described above. The total expected cost is broken down into the following terms:

- Startup cost: $\mathrm{SU} = \sum_{t\in T}\sum_{g\in G} c^{\mathrm{SU}}_{gt}$.
- Shutdown cost: $\mathrm{SD} = \sum_{t\in T}\sum_{g\in G} c^{\mathrm{SD}}_{gt}$.
- Day-ahead energy cost: $\text{DA-E} = \sum_{t\in T}\sum_{g\in G} C^{\mathrm{D}}_{g} p^{\mathrm{D}}_{gt}$.
- Day-ahead reserve capacity cost: $\text{DA-R}= \sum_{t\in T}\sum_{g\in G} \left(C^{\mathrm{CU}}_{g} c^{\mathrm{U}}_{gt} + C^{\mathrm{CD}}_{g} c^{\mathrm{D}}_{gt}\right)$.
- Real-time cost: $\mathrm{RT}=\sum_{\omega\in\Omega}\pi_\omega \sum_{t\in T}\Bigg(\sum_{g\in G^{\mathrm{D}}} \left(C^{\mathrm{DU}}_{g} r^{\mathrm{U}}_{gt\omega} - C^{\mathrm{DD}}_{g} r^{\mathrm{D}}_{gt\omega}\right) + \sum_{n\in N} C^{\mathrm{UD}} p^{\mathrm{UD}}_{nt\omega}$.
- Post-contingency cost: $\mathrm{PC}=\sum_{\omega\in\Omega}\pi_\omega \sum_{t\in T}\sum_{\xi\in\Xi^{\mathrm{OS}}} \rho_\xi \Bigg(\sum_{g\in G^{\mathrm{I}}} C^{\mathrm{GS,F}} p^{\mathrm{GS,F}}_{gt\omega\xi} + \sum_{n\in N} C^{\mathrm{UD}}\Bigg(p^{\mathrm{UD,F}}_{nt\omega\xi} + \sum_{c\in C}\tau_c p^{\mathrm{UD,PC}}_{nt\omega\xi c}\Bigg)\Bigg)\Bigg)$. Note that post-contingency costs, PC, are computed enforcing the obtained scheduling variables in the 100 frequency scenarios that are generated out-of-sample.

We observe that the sum of all pre-contingency costs, SU+SD+DA-E+DA-R+RT, in the proposed model SCSUC+FD is higher than that obtained from model SCSUC in all analyzed cases. This higher cost is compensated in most of the cases by a smaller post-contingency expected cost in SCSUC+FD. It is also observed that the post-contingency costs grow as the frequency deviation limits decrease and the renewable capacity increases. We notice that the decrease of the day-ahead energy costs (DA-E) caused by increasing the penetration of renewable energies is much smaller if a tight frequency limit is enforced ($\Delta f_{\max} = 0.25$ Hz) and frequency deviations are considered in the pre-contingency state. For instance, if RPF=5, decreasing $\Delta f_{\max}$ from 0.50 to 0.25 causes that the day-ahead energy costs increase 8.1 and 5.5% for SCSUC+FD and SCSUC models, respectively. Note that the post-contingency costs are always smaller when the model SCSUC+FD is used.

Table 1: Expected costs (k€)

$\Delta f_{\max}$ (Hz)	RPF (pu)	Model	SU (k€)	SD (k€)	DA-E (k€)	DA-R (k€)	RT (k€)	PC (k€)	Total (k€)
0.50	1	SCSUC+FD	23.83	0.56	621.87	3.64	0.17	1.06	651.13
		SCSUC	23.83	0.56	622.42	3.66	-0.25	4.47	654.69
	5	SCSUC+FD	19.74	0.45	436.10	4.71	1.37	0.63	467.09
		SCSUC	19.47	0.43	435.50	4.76	1.47	6.03	467.66
0.25	1	SCSUC+FD	23.39	0.51	624.42	3.64	0.75	2.71	655.42
		SCSUC	24.06	0.48	623.98	3.76	0.13	8.61	661.02
	5	SCSUC+FD	24.42	0.77	471.30	2.61	20.43	4.63	523.57
		SCSUC	23.78	0.70	459.49	3.39	6.01	21.74	515.11

Table 2 provides the probability of the frequency to be equal to its lower limit when the failure of less costly thermal unit (unit 6) occurs. Note that the failure of this unit has been selected because it is committed in all periods of the considered planning horizon in all analyzed cases. This table also shows the expected unserved demand considering all contingencies. On one hand, it is observed that the probability of the deviation of the frequency to be equal to its lower limit increases significantly as the frequency deviation limit decreases. It is also noted that this probability is much lower when the model SCSUC+FD is used. As the renewable penetration increases, two opposite effects can be observed. First, since part of the production of conventional units is replaced by the additional renewable power production, the failures of conventional units have associated a smaller amount of lost energy. In other words, the failure of a unit working at 50% of its capacity is, a priori, less harmful than the failure of the same unit working at 100% of its capacity. Besides, as the renewable power capacity increases, the number of power units able to provide frequency regulation decreases. This implies a reduction in the power system ability to respond to frequency variations. Considering the above, Table 2 shows that, if unit 6 fails, the probability of experiencing a frequency deviation equal to the limit decreases as the renewable penetration increases. The reason explaining this result is that the production of unit 6 is reduced as the renewable production increases. Therefore, if unit 6 fails, the energy that has to be supplied in the primary response by the rest of units to supply the lost generation decreases and, therefore, the probability of experiencing a frequency deviation equal to the limit is also reduced. In the case of the total expected unserved demand, if model SCSUC is used, we observe that its value increases significantly as the renewable power capacity increases. However, when model SCSUC+FD is used, the expected unserved demand moderately increases ($\Delta f_{\max} = 0.25$ Hz) or even slightly decreases ($\Delta f_{\max} = 0.50$ Hz). Finally, observe that the expected unserved demand is much lower when the proposed model is used.

Table 2: Post contingency results

$\Delta f_{\max}$ (Hz)	RPF (pu)	Model	P($\Delta f^{\mathrm{PC}}_{t\omega\xi 6} = -\Delta f_{max}$) (%)	Expected unserved demand (MWh)
0.50	1	SCSUC+FD	3.4	0.21
		SCSUC	6.8	0.89
	5	SCSUC+FD	1.4	0.13
		SCSUC	2.2	1.21
0.25	1	SCSUC+FD	7.3	0.54
		SCSUC	15.0	1.72
	5	SCSUC+FD	5.1	0.93
		SCSUC	5.4	4.35

4.3. One-year case study

In this subsection, a yearly economical appraisal of the results provided by the proposed formulation is carried out. For each day, 10 demand, wind an solar PV scenarios are generated on the basis of the actual data reported for 2015. As described in Section 4.1, 3 values of frequency in the pre-contingency state are considered. The resulting scheduling is tested in an out-of-sample set of 100 frequency scenarios for each analyzed day. In this case, SCSUC+FD and SCSUC models are tested for $\Delta f_{\max} = 0.5$ and RPF=1.

The obtained results are represented in Figure 5. Figure 5a provides the total expected cost per day obtained from the SCSUC+FD model. For the sake of clarity, daily values in all subfigures of Figure 5 are increasingly ordered. Figure 5a represents the daily expected total cost in SCSUC+FD model. The average daily expected cost obtained by this model is 631.8 k€. Figure 5c shows the relative error of the total cost obtained from SCSUC with respect to SCSUC+FD. In this figure we can observe that the total cost obtained by SCSUC+FD model is smaller than that obtained from SCSUC model in 83% of the considered days. This result indicates that considering a small number of scenarios for modeling the pre-contingency frequency in the scheduling model is enough to achieve a reduction of the expected costs in most of the days. The expected unserved demand is represented in Figure 5b. The average unserved demand obtained by the SCSUC+FD model is 2.3 MWh, that is 85% smaller than that resulting from using the SCSUC model. Figure 5d depicts the variation of the expected unserved demand of SCSUC with respect to SCSUC+FD. From this figure we can conclude that the unserved demand resulting from the SCSUC+FD model is always smaller than that obtained from the SCSUC model.

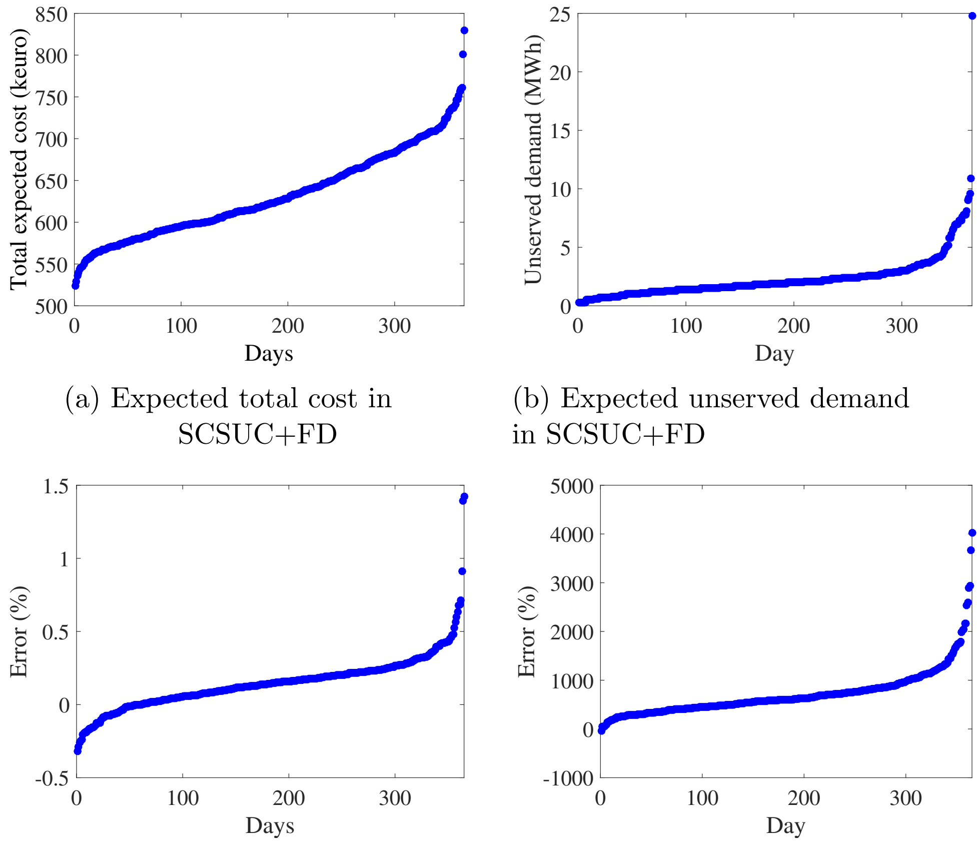

(a) Expected total cost in SCSUC+FD

(b) Expected unserved demand in SCSUC+FD

(c) Variation of the expected total cost of SCSUC with respect to SCSUC+FD

(d) Variation of the expected unserved demand of SCSUC with respect to SCSUC+FD

Figure 5: One-year results

Figure 6 provides the computational performance of the solution procedure described in Section 3.3 for the one-year case study. Figure 6a shows the number of iterations needed to obtain the optimal solution. Observe that in 361 of the 365 days of the year only two iterations are needed to obtain a solution satisfying the pre-fixed tolerance. On the other hand, 3 days need

3 iterations and only one day requires 4 iterations. Figure 6b represents the solution time needed by each iteration in each day. Observe that the average solution times obtained by iterations 1, 2, 3 and 4 are 17, 104, 345 and 106 seconds, respectively. Observe that these solution times are reasonable for a daily operation problem as the one analyzed in this paper. Table 3 provides the number of constraints and number of continuous and binary variables of SCSUC+FD in each iteration of the solution procedure. It must be stressed that the number of binary variables remains constant as the iteration counter grows. This causes that the solution times be reasonable for a day-ahead scheduling, as shown in Figure 6b.

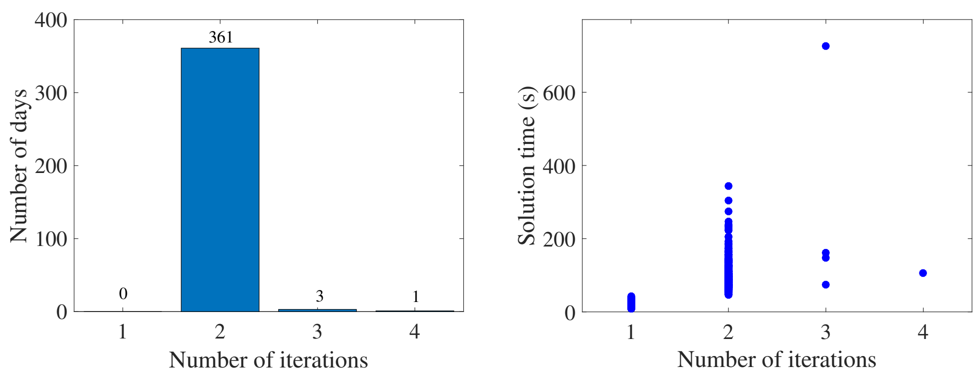

(a) Number of iterations

(b) Solution time per iteration

Figure 6: Computational performance

Table 3: Computational size

	Iteration			
	1	2	3	4
Constraints ($\times 10^3$)	177.9	233.5	289.3	344.9
Continuous variables ($\times 10^3$)	68.9	80.6	92.4	104.2
Binary variables	576	576	576	576

5. Conclusions

In this paper, the influence of the variability of the steady-state pre-contingency frequency in the day-ahead energy and reserve scheduling of small-size power systems has been analyzed. For this purpose, a security-constrained stochastic unit commitment model that considers steady-state frequency variations and PFC has been proposed. This model is formulated as a two-stage stochastic programming problem in which demand, renewable power availability and frequency variations are characterized as random variables. The application of the proposed model is of special interest for small-size power systems and provides the day-ahead energy and reserve capacity schedules.

The case study shows the impact of experiencing off-nominal frequency values on the day-ahead market scheduling. In particular, the numerical results suggest that modeling frequency fluctuations using a small number of scenarios in the day-ahead market reduces significantly the unserved demand after contingency at the expense of a more expensive schedule of energy and spinning reserve capacities. In this sense, the one-year simulation performed in the Lanzarote-Fuerteventura power system states that the unserved demand after contingency is reduced 85% if the proposed model is used. Additionally, the out-of-sample analysis shows that the probability of experiencing high frequency deviations is much smaller if the proposed formulation is used.

6. Acknowledgments

Miguel Carrión and Rafael Zárate-Miñano are supported by the Ministry of Economy and Competitiveness of Spain under Project DPI2015-71280-R MINECO/FEDER, UE. Federico Milano is supported by Science Foundation Ireland under the Investigator Programme award, project AMPSAS, grant no. SFI/15/IA/3074.

References

[1] Mele FM, Ortega Á, Zárate-Miñano R, Milano F. Impact of variability, uncertainty and frequency regulation on power system frequency distribution, in Power Systems Computation Conference (PSCC) 2016;1–8.

[2] Du P, Makarov Y. Using disturbance data to monitor primary frequency response for power system interconnections. IEEE Trans. Power Systems, vol. 29, no. 3, pp. 1431-1432, May 2014.

[3] Ingleson J, Allen E. Tracking the eastern interconnection frequency governing characteristic. Proc. 2010 IEEE Power Eng. Soc. General Meeting, Jul. 2010, pp. 1-6.

[4] European Commission. Clean Energy for All Europeans. Available at https://ec.europa.eu/energy/en/topics/energy-strategy-and-energy-union/ clean-energy-all-europeans (accessed on May 2020)

[5] European Parliament and of the Council. Regulation (EU) 2019/941 on risk-preparedness in the electricity sector and repealing Directive 2005/89/EC. Available at https://eur-lex.europa.eu/legal-

content/EN/TXT/PDF/?uri=CELEX:32019R0941&from=EN (accessed on May 2020)

[6] Wang J, Shahidehpour M, Li Z, Security-constrained unit commitment with volatile wind power generation, IEEE Trans. on Power Systems 2008;23(3):1319–1327.

[7] Bouffard F, Galiana FD. Stochastic security for operations planning with significant wind power generation. IEEE Trans. on Power Systems 2008;23(2):306–316.

[8] Ruiz PA, Philbrick CR, Zak E, Cheung KW, Sauer PW. Uncertainty Management in the Unit Commitment Problem. IEEE Trans. on Power Systems 2009;24(2):642–651.

[9] Papavasiliou A, Oren S, O'Neill RP. Reserve requirements for wind power integration: A scenario-based stochastic programming framework. IEEE Trans. on Power Systems 2011;26(4):2197–2206.

[10] Domínguez R, Conejo AJ, Carrión M, Operation of a fully renewable electric energy system with CSP plants. Applied Energy 2014;119:417–430.

[11] Zheng QP, Wang J, Liu AL. Stochastic Optimization for Unit Commitment - A Review, IEEE Trans. on Power Systems 2015;30(4):1913–1924.

[12] Asensio M, Contreras J. Stochastic Unit Commitment in Isolated Systems With Renewable Penetration Under CVaR Assessment. IEEE Trans. on Smart Grids 2016;7(3):1356–1367.

[13] Psarros GN, Nanou SI, Papaefthymiou SV, Papathanassiou SA. Generation Scheduling in Non-Interconnected Islands with high RES penetration. Renewable Energy 2018;115:338–352.

[14] Chang CA, Wu YK, Chen BK. Determination of maximum wind power penetration in an isolated island system by considering spinning reserve. Energies 2016;9:1–16.

[15] Restrepo JF, Galiana FD. Unit commitment with primary frequency regulation constraints, IEEE Trans. on Power Systems 2005;20(4):1836–1842.

[16] Ahmadi H, Ghasemi H. Security-constrained unit commitment with linearized system frequency limit constraints. IEEE Trans. on Power Systems 2014;29(4):1536–1545.

[17] Ela E, Gevorgian V, Tuohy A, Kirby V, Milligan M,O'Malley M. Market designs for the primary frequency response ancillary service – part I: Motivation and design. IEEE Trans. on Power Systems 2014;29(1):421–431.

[18] Javadi M, Amraee T, Capitanescu F. Look ahead dynamic security-constrained economic dispatch considering frequency stability and smart loads. International Journal of Electrical Power & Energy Systems 2019;108:240-251.

[19] Sokoler LE, Vinter P, Baerentsen R, Edlund K, Jorgensen JB. Contingency-Constrained Unit Commitment in Meshed Isolated Power Systems. IEEE Trans. Power Syst. 2016;31(5):3516–3526.

[20] Dvorkin Y, Henneaux P, Kirschen DS, Pandzic H, Optimizing Primary Response in Preventive Security-Constrained Optimal Power Flow. IEEE Systems Journal 2018;12(1):414–423.

[21] Pascal M, Rachid C, Alexandre O. Optimizing a battery energy storage system for frequency control application in an isolated power system. IEEE Trans. Power Systems 2009; 24(3):1469–1477.

[22] Morales JM, Conejo AJ, Liu K, Zhong J. Pricing Electricity in Pools with Wind Producers. IEEE Trans. Power Systems 2012;2(3):1366-1376.

[23] Tan Z, Li X, He L, Li Y, Huang J. Primary frequency control with BESS considering adaptive SoC recovery. International Journal of Electrical Power & Energy Systems 2020;117:105558.

[24] Carrión M, Domínguez R, Cañas-Carretón M, Zárate-Miñano R. Scheduling isolated power systems considering electric vehicles and primary frequency response. Energy 2019;168:1192–1207.

[25] Karbouj H, Hussain Rather Z, Flynn D, Qazi HW, Non-synchronous fast frequency reserves in renewable energy integrated power systems: A critical review. International Journal of Electrical Power & Energy Systems 2019;106:488-501.

[26] Birge JR, Louveaux F. Introduction to Stochastic Programming. New York: Springer-Verlag, 1997.

[27] Conejo AJ, Carrión M, Morales JM. Decision Making Under Uncertainty in Electricity Markets. New York: Springer, 2010.

[28] Ardakani AJ, Bouffard F. Identification of Umbrella Constraints in DC-Based Security-Constrained Optimal Power Flow. IEEE Trans. Power Systems 2013;28(4):3924–3934.

[29] Spanish Network Operator (Red Eléctrica de España), available at: http://www.ree.es.

[30] Heitsch H, Rømisch W. Scenario reduction algorithms in stochastic programming. Comp. Opt. and App. 2003;24(2):187–206.